Journal of
Mechanical
Science and
Technology

Journal of Mechanical Science and Technology 21 (2007) 764~771

Acoustic Properties Associated with Nozzle Lip Thickness in Screeching Jets

Yongseok Kim[a,*], Duck Joo Lee

[a]*School of Mechanical and Aerospace Engineering, Sunchon National University 315 Maegok, Suncheon, 540-742 Korea*
Department of Aerospace Engineering, Korea Advanced Institute of Science and Technology, Korea

(Manuscript Received October 27, 2006; Revised April 6, 2007; Accepted April 9, 2007)

Abstract

Imperfectly expanded supersonic jets generate discrete frequency sound known as screech tones. In the low supersonic Mach number, the screech phenomenon is axisymmetric. In this study the effect of nozzle lip thickness on the axisymmetric jet screech is investigated both by screech scattering computation and screeching jet simulation. The conservative form of the axisymmetric Euler equations in generalized coordinates are used to simulate a scattering problem and the Reynolds-Averaged Navier-Stokes equations with the modified Spalart-Allmaras turbulence model is employed for screeching jet simulation. Numerical results of scattered directivity pattern in scattering computation will be reported. Influence of the nozzle lip thickness on the momentum thickness, shock-cell spacing and screech tone wavelength is examined.

Keywords: Supersonic jet; Screech tone; Nozzle lip thickness; Screech tone scattering; Directivity pattern

1. Introduction

Under/over-expanded supersonic jets emit turbulent mixing noise, broadband shock-associated noise, as well as screech tones under certain conditions. The mixing noise is directly associated with large-scale structures, or instability waves, in the jet shear layer and the broadband shock-associated noise is occurred by the interaction of instability waves with shock cell structure in the jet plume. The screech tone is known to be generated by feedback loop involving instability wave, reflected wave and shock cell near the nozzle lip (Powell, 1953; Tam, 1995). Screech tone is more critical not only because of general noise-reduction concerns, but also because of acoustic fatigue to structures. Better understanding of the screech feedback mechanism and better prediction of the screech amplitude are necessary in order to suppress screech tones without the loss of performance. The main part of screech tones generated by shock-instability interactions propagate upstream and impinge on the nozzle lip wall, and the reflected and scattered waves interact with a thin shear layer of the jet. This process amplifies the instability waves, leading to generation of strong screech tones. To identify the feedback loop mechanism more clearly and predict the amplitude of screech tones more accurately, both experimental and numerical approaches have been taken, including the pioneering work by Powell (Powell, 1953; Tam et al., 1997; Raman, 1998; Shen and Tam, 2000; Loh et al.;2001).

Screech tones are known to be sensitive to changes in the external environment of the jet and the presence of sound reflection surfaces. Effect of nozzle lip thickness on screech tone intensity in the view of the screech suppression was observed first by Norum (Norum, 1983). There is good reason to believe that

*Corresponding author. Tel.: 82 61 750 3957
E-mail address: yongskim@sunchon.ac.kr

the nozzle lip is definitely an acoustic reflection surface. The reflected and scattered waves by the lip surface are important to the excitation of the instability wave that leads to the screech tone. A more rigorous measurement of nozzle lip thickness effect was carried out by Ponton and Seiner(1992). Recently, Aoki and his colleagues(2006) showed experimentally nozzle lip thickness affects the acoustic characteristics of the screech tones strongly in the case of over-expanded jets, while for under-expanded jets, the effects of nozzle lip thickness on the screech tone frequency is relatively small.

The objective of the present paper is to examine how the nozzle lip thickness affects the screech tone and to provide numerical data for understanding feedback mechanism of the screech tone by considering both screech scattering problem and screeching jet simulation. Moreover, we focused on the supersonic jet structure to investigate the effect of nozzle lip thickness on the change of momentum thickness, radial velocity profiles and shock-cell spacing. And relations between momentum thickness, shock-cell spacing and screech tone wavelength according to the change of nozzle lip thickness will be addressed.

To analyze the scattered pattern by screech tones an acoustic scattering problem by a nozzle lip is taken up, where a jet mean flow is not considered. This scattering problem can be realized by the interaction between plane waves, which represent screech tones, and a nozzle lip wall. A high resolution finite volume essentially non-oscillatory(ENO) scheme is used along with nonreflecting boundary conditions that are crucial to screech tone propagation and scattering computations to accurately capture the amplitude and directivity of generated sounds.

2. Numerical methods

Both appropriate high-resolution numerical schemes and boundary treatment are crucial for the accurate computation of aeroacoustic problems, especially for the screech tone simulation. Since the amplitude variation among the sound waves, the shock cells and the large scale instability waves is very large. The finite volume Modified-Flux-Approach ENO (Essentially Non-oscillatory) schemes coupled with the characteristic boundary conditions are used both to acoustic scattering and to screeching jet computations. The MFA-ENO schemes considered here have been verified by a geometrically complicated system (Kim and Lee, 2001), where the uniform 4^{th}-order accuracy in time and space are achieved both at local extrema of the solutions and in other smooth regions. They can resolve accurately not only a strong discontinuity like a shock-cell or a large-scale vortex, but also the small amplitude of sound waves (Kim and Lee, 2002).

3. Numerical results and discussions

3.1 Screech scattering simulation

In the experiment of Ponton and Seiner(1992), it was reported that increasing the nozzle lip thickness increased the screech tone amplitudes on the nozzle exit lip surface. The purpose of the present study is to demonstrate experimental results and to examine the effect of nozzle lip thickness on screech tone and scattered acoustic fields. Screech tone is well known to be generated by feedback loop. Good understanding of the screech feedback mechanism and better prediction of the screech amplitude are necessary in order to suppress screech tones without the loss of performance.

Screech scattering problem is considered to analyze scattered patterns between screech tone and nozzle lip wall without jet mean flow. The screech tone can be described by plane waves as shown in Fig. 1. Present study focuses on axisymmetric modes of the screech tone. For this purpose, the conservative form of the axisymmetric Euler equations written in generalized coordinates is applied. The computational domain and boundary conditions in the simulation of screech scattering are shown schematically in Fig. 1. The plane waves are provided from the left inlet under the nonreflecting transparent characteristic boundary condition that enables the source to be transparent and

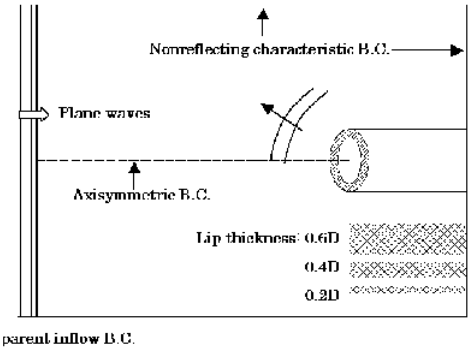

Fig. 1. Schematic diagrams showing the screech tone scattering simulation and considered nozzle lip thickness.

prevents the plane waves from being reflected at the inlet boundary. At the jet axis, the symmetry boundary condition is used. In the present simulation, the screech wavelength and sound pressure level were set to be 1.6 D (D is nozzle diameter), and 135 dB, respectively. The incident plane waves with sound pressure p_i has frequency f and pressure amplitude p_{0i}.

$$p_i = p_{0i} \cdot \sin(2\pi ft) \tag{1}$$

These sound pressure waves are emitted from the left side of the computational domain, which interact with the nozzle lip wall. The scattering process is usually characterized by incident wave p_i, total pressure p_t and scattered wave pressure p_{scat}, where p_{scat} can be computed from p_t and p_i as

$$p_{scat} = p_t - p_i \tag{2}$$

Figure 2 shows the incident, total and scattered fields of numerical solutions for 0.4 D lip thickness. The scattered acoustic directivity is clearly shown in Fig 2-(c). It reveals that upstream propagating waves which are reflected by nozzle lip wall are dominant. It can amplify shear layer fluctuations near the nozzle exit, eventually screech tone amplitude. As mentioned before, one of the important things in scattering simulation is boundary condition. In particular, inlet source boundary should be treated carefully owing to reflections between entering acoustic sources and outgoing waves. The nonreflecting transparent boundary condition considered here seems to work well at the inlet boundary, where the reflection of acoustic waves is not observed.

Figure 3 shows comparison of the scattered pressure fields of three nozzle lip thickness. The more nozzle lip thickness is increased, reflected and scattered amplitude is also increased. This tendency is consistent with experimental results, which is more clearly explained by the pressure distributions along the x-axis in Fig. 4 and y-axis in Fig. 5. It is concluded that the thicker nozzle lip produces more intense reflected waves by interacting between incident screech waves and nozzle lip wall. Three dimensional view of scattered pressure contour in Fig. 6 shows more easily that the scattered directivity is upstream(x-axis) dominant. In the next section, nu-

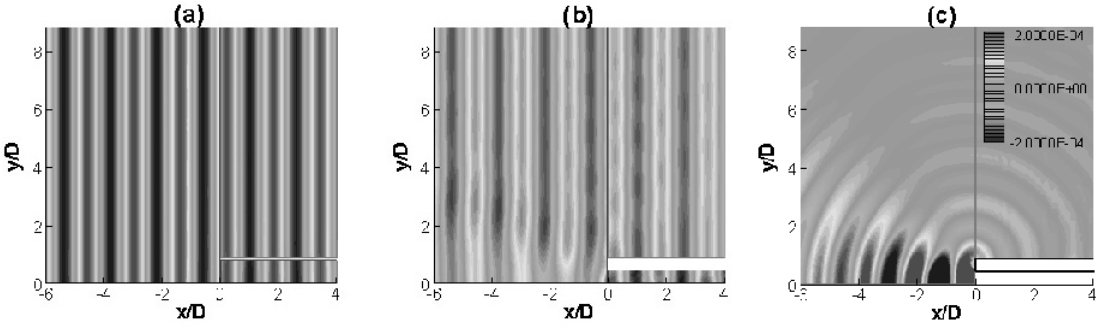

Fig. 2. Instantaneous pressure fields in screech tone scattering problem. (a) Incident field ,(b) Total field (c) Scattered field (Nozzle lip thickness: 0.4D).

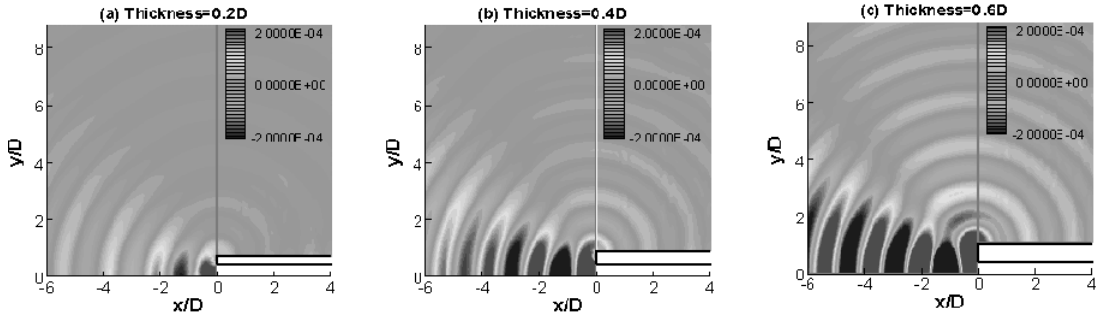

Fig. 3. Comparison of instantaneous scattered pressure fields according to change of the nozzle lip thickness: (a) 0.2 D, (b) 0.4 D, (c) 0.6 D.

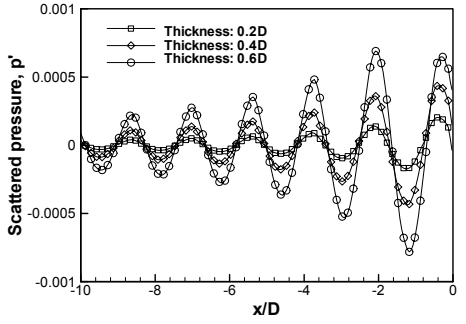

Fig. 4. Comparison of pressure distribution along the x-axis (y=0.5 D).

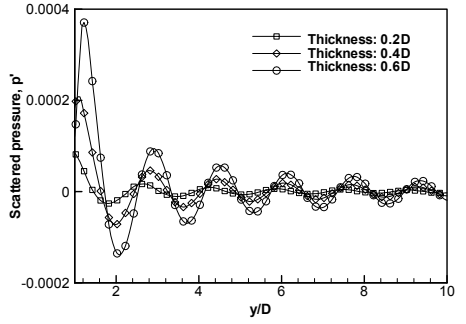

Fig. 5. Comparison of pressure distribution along the y-axis (x=0.0 D).

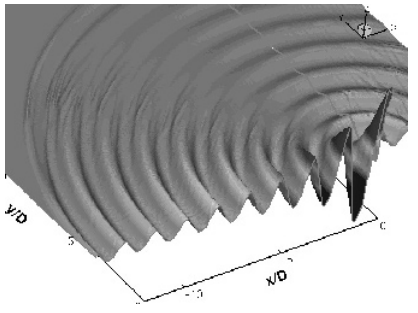

Fig. 6. Three dimensional view of the scattered pressure contour showing an acoustic directivity.

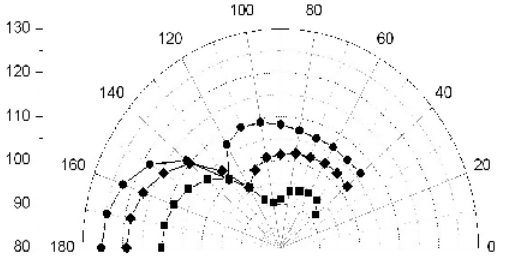

Fig. 7. Comparison of sound pressure level at the r=5D showing directivity patterns (Nozzle lip thickness: ■=0.2D, ◆=0.4D, ●=0.6D)

merical simulation results of the screeching jet with three nozzle lip thickness are discussed in detail. Figure 7 represent comparison of SPL(sound pressure level) at the position of r=5D. Directivity patterns plotted from scattered pressure data show two lobes and the magnitude of reflected waves is quite different. We can estimate that thick nozzle lip can produce more intense screech tone sound in a supersonic jet flow.

3.2 Supersonic jet and screech tone simulation

In this section, an axisymmetric jet is simulated at a fully expanded Mach number of 1.2 with three nozzle lip thickness to examine the effect of nozzle lip thickness on screech tone. The operating condition of the jet is fully described by specifying the reservoir to ambient pressure and temperature ratios. The pressure ratio is expressed in terms of the jet Mach number, M_j, which would be the exit Mach number of the corresponding perfectly expanded jet as below:

$$M_j = \left\{ \frac{2}{(\gamma-1)} \left[\left(1 + \frac{M_e^2(\gamma-1)}{2} \right) \cdot \left(\frac{p_e}{p_\infty} \right)^{\frac{\gamma-1}{\gamma}} - 1 \right] \right\}^{\frac{1}{2}} \quad (3)$$

In order to consider the axisymmetric screeching jet, the axisymmetric RANS(Reynolds-Averaged Navier-Stokes) equations are used with the modified Spalart-Allmaras turbulence model (Spalart and Allmaras, 1992). In this model, the eddy viscosity is computed through a partial differential equation. In particular, the eddy viscosity ν_T is computed by an intermediate variable $\bar{\nu}$ through the following relation:

$$\nu_T = \bar{\nu} f_{v1}(\chi), \ \chi = \frac{\bar{\nu}}{\nu} \quad (4)$$

where f_{v1} is a damping function. The intermediate variable $\bar{\nu}$ is computed by solving a differential transport equation that can be written in compact form as follow:

$$\frac{D\bar{\nu}}{Dt} = \frac{1}{\sigma}\left[\nabla \cdot \left((\nu + \bar{\nu}) \nabla \bar{\nu} + c_{b2} (\nabla \nu)^2 \right] + c_{b1} \bar{S} \bar{\nu} (1 - f_{t2}) - \left[c_{w1} f_w - \frac{c_{b1}}{\kappa^2} f_{t2} \right] \left[\frac{\bar{\nu}}{d} \right]^2 + f_{t1} (\Delta q)^2 \quad (5)$$

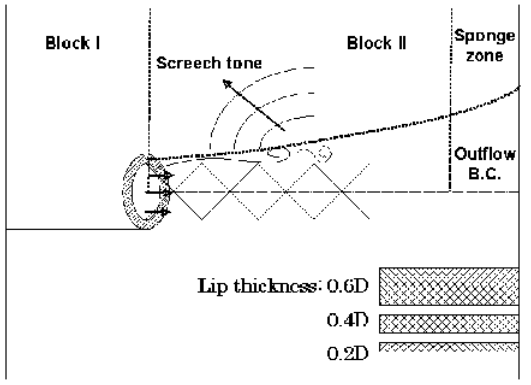

Fig. 8. Schematics of computational domain and boundary conditions.

where the various functions and constants are reported in the reference (Klaus, 2000). In the present simulation, the constants in the transport equation are used as follow:

$$\sigma = 2/3,\ c_{b1} = 0.1355,\ c_{b2} = 0.622$$
$$c_{w1} = \frac{c_{b1}}{\kappa^2} + (1 + c_{b2})/\sigma,\ c_{w2} = 0.3,\ c_{w3} = 2,\ \kappa = 0.41$$
$$c_{v1} = 7.1,\ c_{t1} = 1.0,\ c_{t2} = 2.0,\ c_{t3} = 1.1,\ c_{t4} = 2.0 \quad (6)$$

It should be noted that the trip function f_{t1} and the function f_w are neglected in the screech jet simulation. Moreover, the coefficient c_{b1} is adjusted depending on screech jet Mach number.

Figure 8 shows schematics of computational domain and boundary conditions. Non-reflective boundary conditions are applied at the left boundary and in outer boundary regions. In the downstream boundary region where $M_a \geq 0.001$, the outflow boundary conditions are implemented. A buffer, or sponge, zone is used to eliminate any small, re-maining numerical reflections from the downstream outflow boundary. At the nozzle exit, the flow variables are taken to be uniform corresponding to those at the exit of a convergent nozzle. All nondimensional variables are given as follows:

$$\rho_e = \frac{\gamma(\gamma+1)p_e}{2T_r}$$
$$P_e = \frac{2}{\gamma}\left[\frac{2+(\gamma-1)M_j^2}{\gamma+1}\right]^{\frac{\gamma}{\gamma-1}} \quad (7)$$
$$u_e = \left(\frac{2T_r}{\gamma+1}\right)^{1/2},\ v_e = 0$$

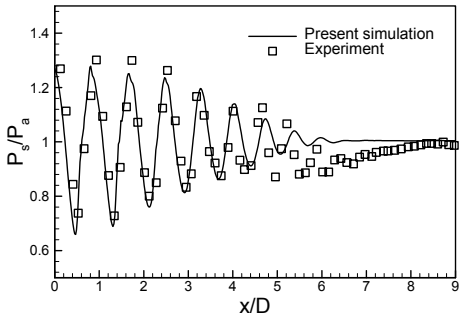

Fig. 9. Centerline pressure comparison between the present calculation and experimental data by Norum & Brown (1993) for a cold jet (Nozzle lip thickness: 0.4D, $M_j = 1.2$).

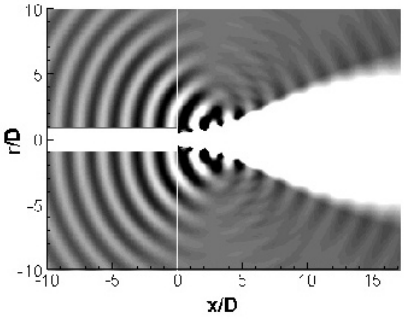

Fig. 10. Instantaneous density field from the numerical simulation showing the generation and propagation of screech tone ($M_j = 1.2$, t/D=0.4)

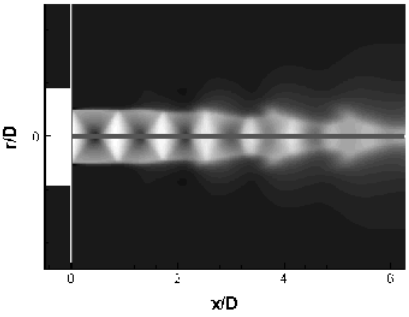

Fig. 11. Density contour showing shock cell structure of a screeching jet. ($M_j = 1.2$, t/D=0.4).

where γ is equal to 1.4. T_r is the reservoir temperature, which is set to 1 for the cold jet assumption. As for the turbulence model, the turbulent viscosity at the nozzle exit is set to zero.

In the previous section, it was found that thick nozzle lip can generate more intense reflected pressure waves than thin one, which propagate mainly into axial upstream direction. We performed screeching jet simulation considering with a mean flow. To verify an accuracy of the present numerical

methods, computed result is compared with existing experimental data. Figure 9 presents the time-averaged pressure along the jet axis at $M_j = 1.2$. The instantaneous density field in Fig. 11 after the initial transient has propagated out of the computational domain shows the generation and propagation of screech tone. As we can see, the screech tone radiates principally in the upstream direction and it interacts with a nozzle lip. Acoustic disturbance impinging on the nozzle lip where the jet mixing layer is thin and so receptive to external perturbation excite the jet shear layer and instability wave. It propagates downstream with growing amplitude and interacts with the shock cells. The interaction leads to the emission of additional acoustic waves. In this way, the feedback loop is closed.

One important issue regarding the screech tone is shock cell structure. We can see the shock cell structure clearly from the density contour in Fig. 11. The shock cell spacing and shock amplitude have to be calculated accurately in order to ensure the accuracy of both screech frequency and amplitude. The numerical result obtained in this study is compared with the experimental data by Norum & Brown (1993) in Fig. 9. The first five shocks show good agreement between the simulation and the experiment.

Figure 12 presents acoustic pressure time history on the nozzle lip surface(r=0.65D). It is measured from upstream propagating screech waves and indicates that the thicker nozzle lip generates more intense screech tone, which was expected from scattering problem.

We plotted velocity vector field in Fig. 13 to examine radial velocity distributions and influence of turbulent mixing. It is found that the initial velocity profiles near the nozzle exit are straight like a top hat. After the x/D is 7, velocity flow field behaves like the Gaussian distributions. In this region, large-scale votices are rolled up strongly and convected to the jet downstream. Due to the vortices convection with high speed, a flow entrainment is occurred from the far field and the turbulent mixing is also enhanced.

Figure 14 shows comparison of radial velocity profiles according to the change of nozzle lip thickness at several axial locations(x/D=0.02 ~ 4). In the case of nozzle lip thickness 0.4D and 0.6D, radial velocity profiles are almost same, however it is found that the velocity is increased after D/x=2 in the case of 0.2D case. Because the change of velocity profiles is closely related to the momentum thickness, we

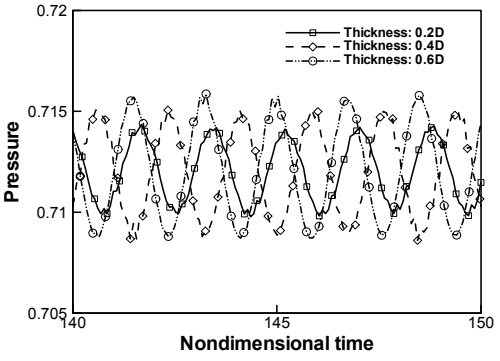

Fig. 12. Comparison of acoustic pressure time history on the nozzle lip wall (r=0.65D).

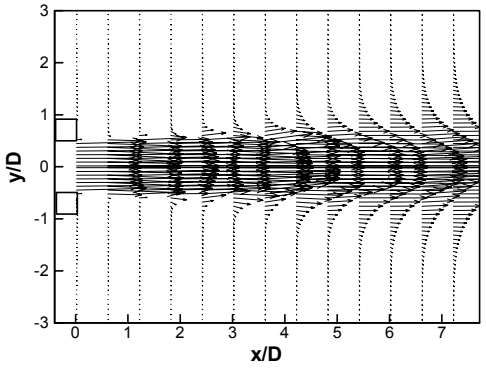

Fig. 13. Instantaneous velocity vector field ($M_j = 1.2$, t/D=0.4).

calculated compressible momentum thickness by following equation

$$\Theta = \int_0^\infty \frac{\rho u}{(\rho u)_0}\left(1 - \frac{u}{u_0}\right) dr \tag{8}$$

where ρu and u represent the mass flow and velocity, and the subscript indicates reference quantities. Ponton and Seiner(1992) used reference quantities as maximum velocities at the radial position because turbulent production is dependent on the velocity gradient. Thus the calculation used for the compressible momentum thickness is

$$\Theta = \int_{R@u_{\max}}^\infty \frac{\rho u}{(\rho u)_{@u_{\max}}}\left(1 - \frac{u}{u_{\max}}\right) dr \tag{9}$$

For the calculation of momentum thickness, mean velocity profiles in Fig. 14 were used.

A momentum thickness comparison of the three lip

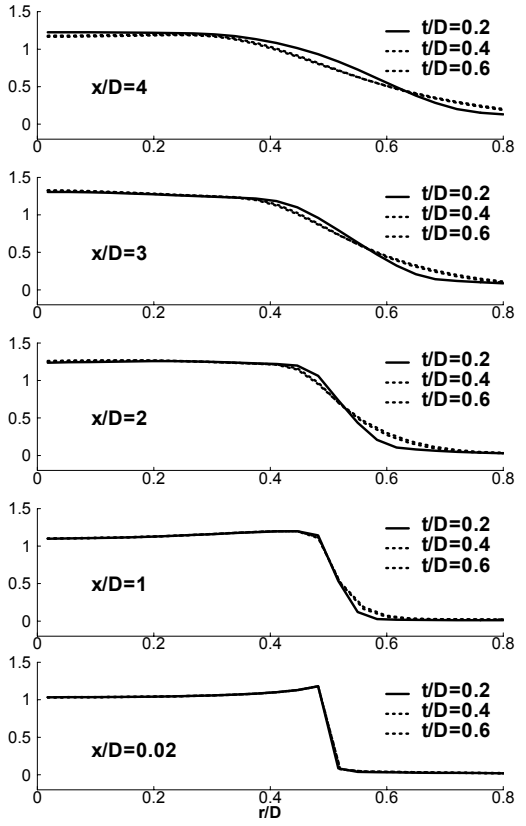

Fig. 14. Comparison of radial velocity profiles at several axial locations.

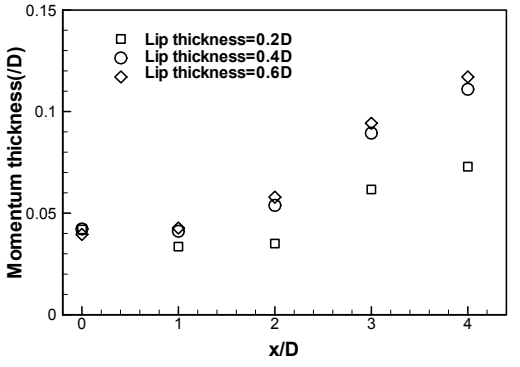

Fig. 15. Comparison of momentum thickness at several axial locations.

thickness, for five axial positions computed, is presented in Fig. 15. While the differences are small in the case of 0.4 D and 0.6 D, it is shown clearly that the momentum thickness is greater for the larger lip thickness in the comparison between 0.2 D and others. It can be easily expected from the comparison of the velocity profiles in Fig. 14. This tendency may indicate greater mixing is occurring for the larger lip thickness.

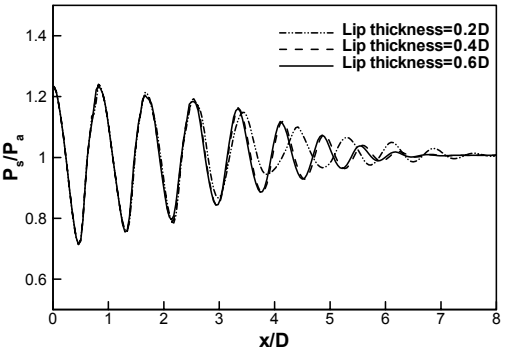

Fig. 16. Comparison of centerline pressure distributions showing the shock-cell spacing.

Figure 16 shows the centerline pressure distributions, which represent the shock-cell spacing. It is found that an increase in momentum thickness cause a reduction in the shock-cell spacing. Moreover, because the wavelength of screech is directly related to the shock-cell spacing, an increase in momentum thickness (due to an increase in lip thickness) causes a decrease in screech wavelength based on the following relation.

$$f_s = \frac{u_c}{L(1+M_c)} \tag{10}$$

where L is shock-cell spacing, u_c, M_c represent convective velocity and Mach number respectively.

4. Conclusion

In this study the effects of nozzle lip thickness on the axisymmetric jet screech are investigated both by scattering computation and screeching jet simulation. To establish the accuracy of the computation results, centerline pressure distribution that reveals shock cell structure and plays key role in determining the screech frequency and amplitude is compared with the experimental data by Norum & Brown. The first five shocks show good agreement between with the simulation and the experiment. It was found that the thicker nozzle lip produces more intense reflected waves by interacting between incident screech waves and nozzle lip wall in scattering computation.

We examined the effect of nozzle lip thickness on the change of momentum thickness, radial velocity profiles and shock-cell spacing and found out that an

increase in momentum thickness cause a reduction in the shock-cell spacing. Moreover, because the wavelength of screech is directly related to the shock-cell spacing, an increase in momentum thickness (due to an increase in lip thickness) causes a decrease in screech wavelength

Acknowledgements

This work was supported by the NURI project of the Ministry of Education & Human Resources Development, Korea in 2007.

References

Aoki. T, Kweon Y. -H, Miyazato. Y, Kim. H. -D and Setoguchi. T, 2006, "An Experimental Study of the Nozzle Lip Thickness Effect on Supersonic Jet Screech Tones," *J. Mechanical Science and Technology*, Vol. 20, No. 4, pp. 522~532.

Kim, Y. S. and Lee, D. J., 2001, "Numerical Analysis of Internal Combustion Engine Intake Noise with a Moving Piston and a Valve," *Journal of Sound and Vibration*, Vol. 241, No. 5, pp. 895~912.

Klaus, A. H., 2000, "Computational Fluid Dynamics Volume III," 4th Edition, pp. 48~50.

Kim, Y. S. and Lee, D. J., 2002, "Computation of Shock-Sound Interaction Using Finite Volume Essentially Non-oscillatory Scheme," *AIAA Journal*, Vol. 40, No. 6, pp. 1239~ 1240.

Loh, C. Y., Hultgren, L. S., and Jorgenson, P. C. E., 2001, "Near Field Screech Noise Computation for an Underexpanded Supersonic Jet by the CE/SE Method," AIAA Paper.

Norum, T. D., 1983, "Screech Suppression in Supersonic Jet," *AIAA Journal*, Vol. 21, No. 2, pp. 235~240.

Norum, T. D. and Brown, M. C., 1993, "Simulated High-Speed Flight Effects on Supersonic Jet Noise," AIAA Paper.

Ponton, M. K. and Seiner. J. M., 1992, "The Effects of Nozzle Exit Lip Thickness on Plume Resonance," *Journal of Sound and Vibration*, Vol. 154, No. 3, pp. 531~549.

Powell, A., 1953, "On the Noise Emanating from a Two-Dimensional Jet above the Critical Pressure," *Aeronautical Quarterly*, Vol. 4, pp. 103~ 122.

Raman G., 1998, "Advances in Understanding Supersonic Jet Screech : Review and Perspective", Progress in Aerospace Science, Vol. 34, pp. 45~106.

Shen, H. and Tam, C. K. W., 2000, "Effects of Jet Temperature and Nozzle-Lip Thickness on Screech Tones", *AIAA Journal*, Vol. 38, No. 5, pp. 762~767.

Spalart, P. R. and Allmaras, S. R., 1992, "A One-Equation Turbulence Model for Aerodynamic Flows," AIAA Paper.

Tam, C. K. W., 1995, "Supersonic Jet Noise," *Annual Review of Fluid Mechanics*, Vol. 27, pp. 17~43.

Tam, C. K. W., Shen, H. and Raman, G., 1997, "Screech Tones of Supersonic Jets from Bevelled Rectangular Nozzles," *AIAA Journal*, Vol. 35, No. 7, pp. 1119~1125.